Single Visit Completeness Optimization
Sarah Hunyadi, Stuart Shaklan, Robert Brown
November 28, 2005

ABSTRACT

The Terrestrial Planet Finder Coronagraph (TPF-C) is a NASA pre-phase-A orbiting telescope with the goal of detecting and characterizing visible and near-IR light reflected from terrestrial planets. We use observational completeness, defined as the fraction of potentially observable planets that are detected, to determine how well the proposed telescope meets the mission goals. Single visit completeness is optimized by selecting the length of observation per target that maximizes the completeness for the ensemble of stars. In this memo we describe the integration time calculations and two approaches to single visit optimization. We also compare the results for different choices of coronagraph sensitivity.

1. INTRODUCTION

The Terrestrial Planet Finder - Coronagraph (TPF-C) is an Origins project in the pre-phase-A stage. It is a proposed space based telescope designed to detect and characterize Earth-like exo-solar planets. There are 1408 potential candidate stars with B-V>0.3 that TPF-C may observe. Around these candidate stars, a so called "habitable zone" or "habisphere" may be defined as the region around the star where liquid water could exist. In the Solar System, this zone exists in the spherical shell defined by the orbits of Venus and Mars (STDT, 2005). The TPF-C mission seeks to search this zone for detection and characterization of exo-solar planets. One measure of how well the mission meets the goal of detection is completeness, defined as the fraction of potential planets in the habisphere that are detected. Single visit completeness, explored in this memo, is the completeness obtained in one observation. The cumulative completeness, which defines the total accumulated completeness, may then be defined as the sum of the completeness values obtained for each visited star.

Brown (2004) defined several types of completeness, including obscurational completeness, the limit imposed by the IWA restrictions and photometric completeness, the limit imposed by instrument sensitivity requirements. The type of completeness explored in this memo is single visit completeness, which includes both the current instrument sensitivity requirements and IWA restrictions. The purpose of this memo is to explore optimized single visit completeness. For single visit completeness, the optimization serves to maximize the total number of detectable planets observed (total accumulated completeness) in a limited integration time. The mission parameters are given in Table 1.

Table 1. Instrument and mission parameters for the TPF-C mission.

2. COMPLETENESS

Each star in the mission plan has a habitable zone. In this memo, this habitable zone exists between 0.7 and 1.5AU for a solar type star[*]. This zone is scaled based on solar luminosity by the rule:

$$0.7\sqrt{L} \le a \le 1.5\sqrt{L} , \tag{1}$$

where a is the semi-major axis of a planet in the habitable zone. In order to model this habitable zone, we populate the habisphere with $N_p = 10,000$ planets in random and evenly distributed orbits with uniformly distributed eccentricities from (0, 0.35). The planet location is defined by 3 Euler angles, ϕ (rotation about the z axis, $0 \le \phi \le 2\pi$), θ (rotation about the x axis, $0 \le \theta \le 2\pi$), and ψ (rotation about the z axis, $0 \le \psi \le \pi$), (Brown, 2004). It is not necessary to include the rotation angle ψ in definition of planetary orbits because it changes neither the separation between the planet and the star nor the phase angle. Additionally, we assume that the inner working angle (IWA) is not a function of azimuth.

---

[*] For future research we use a habitable zone definition of $0.75\sqrt{L} \le a \le 1.8\sqrt{L}$, which is congruent with the SRD (STDT, 2005).
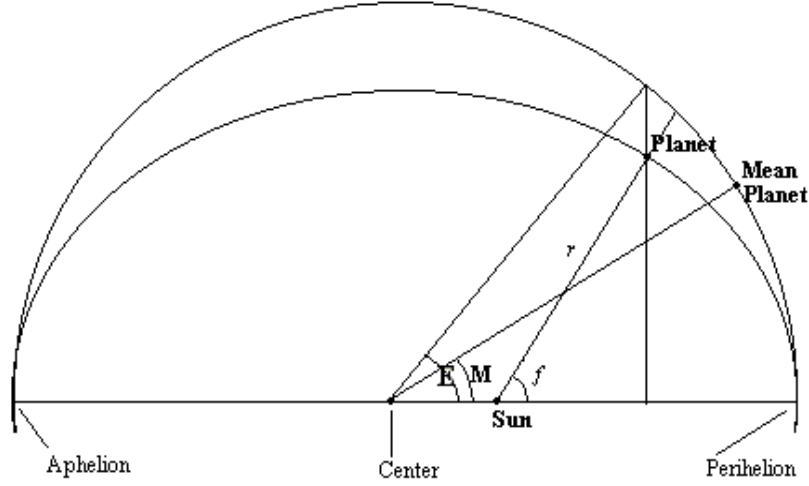
Fig. 1. Diagram of nomenclature for elliptic orbit angles where the line of sight lies in the z-axis and the x and y axes are in the plane of the sky. (courtesy: http://www.frostydrew.org/observatory/courses/orbits/booklet.htm)

For elliptical orbits, the phase is given by:
$$M = E - e \sin E . \tag{2}$$
where M is random on $0 \le M \le 2\pi$, E is the intermediate angle and e is the eccentricity. The true anomaly, f, may then be calculated from the following equations:
$$r = a(1 - e \cos E) \tag{3}$$
$$f = \cos^{-1}\left(\frac{a(1 - e^2) - r}{er} \right) \tag{4}$$
where r is the distance to the planet from the star, a is the semi-major axis and e is the eccentricity. It is this true anomaly is first applied as a projection onto the x and y axes (i.e. the plane of the sky) and then is followed by the z and x rotations. After rotating the coordinate system, the projected distance to the planets is calculated by:
$$r_p = \sqrt{x_{fzx}^2 + y_{fzx}^2} , \tag{5}$$
where x_{fzx} is the rotated x coordinate (after the true anomaly projection and two rotations) and y_{fzx} is the rotated y coordinate (after the true anomaly projection and two rotations). The planetary illumination is dependent on the orbital position of the planet relative to the star. The phase angle is given by:
$$\beta = \cos^{-1}\left(\frac{y_{fz} \sin(\theta)}{r} \right), \tag{6}$$
where y_{fz} is the rotated y coordinate after the true anomaly projection and z rotation. Assuming a Lambert phase function, the fraction of observed, relative planet brightness is given by:
$$\Phi_l(\beta) = \frac{(\sin(\beta) + (\pi - \beta)\cos(\beta))}{\pi}, \tag{7}$$

where $\Phi_l(\beta)=1$ is the fully illuminated planet. The magnitude of the planet is a function of the fraction of planetary illumination multiplied by the albedo (p_e) of the planet. The magnitude of the planet also depends on the planet's distance from the star and the planet's orientation when viewed from Earth. The difference between the magnitude of the planet and the magnitude of the star, or delta magnitude (Δmag), is given by:

$$\Delta mag_e = -2.5\log(r_e^2) - 2.5\log(p_e\Phi_l(\beta)) + 5\log r ,\qquad (8)$$

where r_e is the radius of the earth in AU and p_e is the albedo of earth. The determination of Δmag and r_p for each of the N_p planets leads to a plot of projected planet distance vs. Δmag. This figure was first presented by Brown (2005) and is recreated for the orrery of N_p planets (Fig. 2).
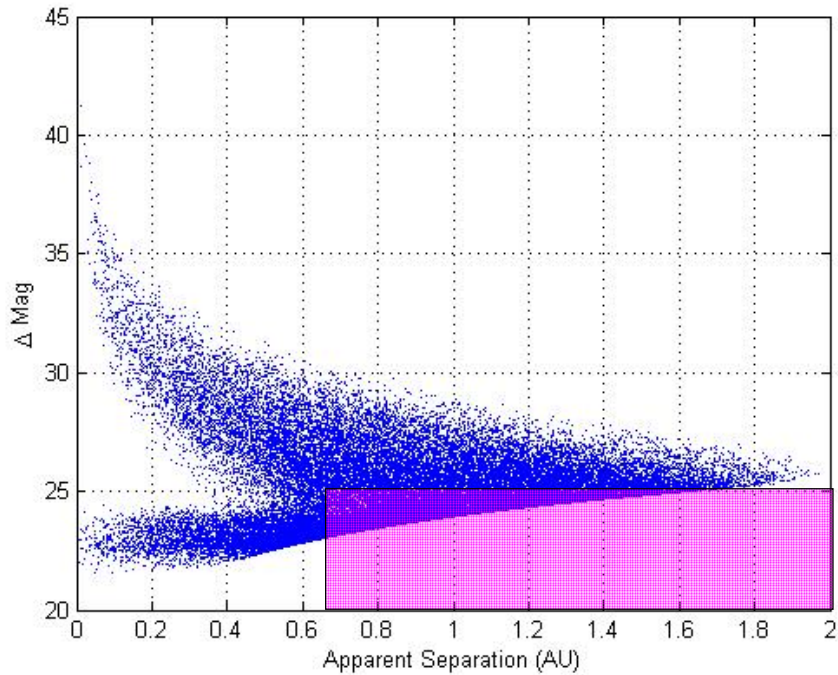

Fig. 2. The planetary probability density distribution for earth like planets in habitable orbits for a solar type star (Hipparcos#62207). The pink box indicates the current sensitivity requirements for the TPF-C mission.

For lower luminosity stars, the shape of the distribution in Fig. 2 stays the same, but moves down in the ordinate direction and is compressed in the abscissa towards lower apparent separation. For high luminosity stars, the distribution shifts up in Δmag and extends further out in projected IWA. The TPF-C mission has a maximum Δmag and a minimum IWA set by the telescope dimension and stability parameters. These parameters define a box (Fig. 2), the height of which is the Δmag sensitivity limit. The baseline Δmag sensitivity limit is $\Delta mag = 25$.

The left side of the pink box is the IWA, which is currently set to $4\lambda/D$, giving an IWA = 57.0x10^{-3} arcsec. However, the IWA is effectively IWA = 65.5x10^{-3} arcsec after accounting for the shape of the mask and telescope rotations. The projected inner working angle or minimum apparent separation (the x-axis in Fig. 2) is defined as the IWA multiplied by the distance to the star in parsecs.

The limiting Δmag and projected IWA define a box, as shown in Fig. 2. The number of planets (N_b) that fall within the box divided by the total number of planets (N_p) is the single visit completeness:

$$Comp = \frac{N_b}{N_p},$$ (9)

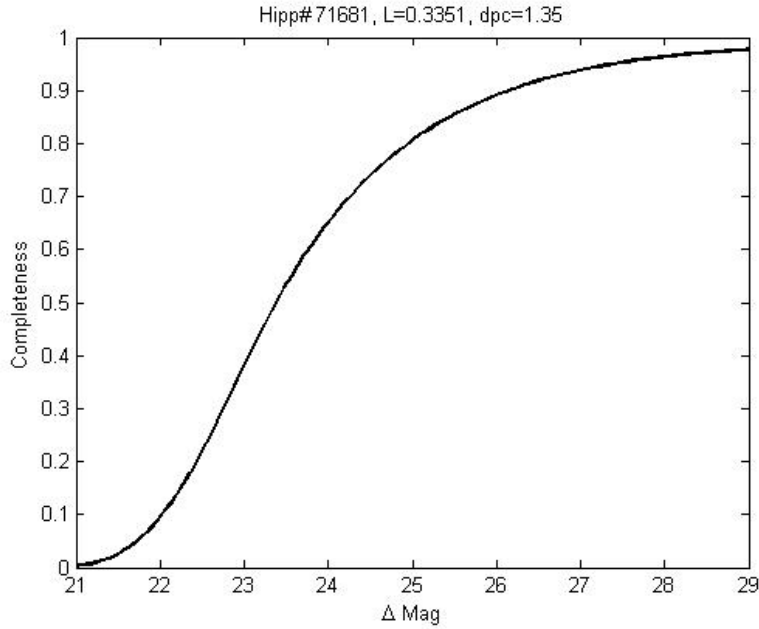In Fig. 3 we plot the completeness as a function of Δmag limit for a typical star.

Fig. 3. Completeness vs. Δmag. As Δmag increases, completeness approaches the maximum value set by the IWA (observational completeness).

3. INTEGRATION TIMES

The Δmag, and therefore completeness, also varies with integration time. Integration time calculations are given in Brown (2005) as a combination of noise count contributions that are dependent on the optical system throughput. The TPF-C telescope is composed of an optical system, including a Lyot stop and an image plane mask. The total system throughput is given by:

$$T_{tot} = t_o t_m t_{Ly} \eta,$$ (10)

where t_o is the optical throughput with the Lyot stop and mask removed, t_m is the mask throughput, t_{Ly} is the Lyot throughput and η is the CCD quantum efficiency.

The telescope area is carried explicitly in each of the noise count terms. Detected photon counts can be given as:

$$C = FA\tau \qquad (11)$$

where F is detected flux, τ is integration time and A is the telescope area give by:

$$A = \frac{1}{y}\frac{\pi}{4}D^2, \qquad (12)$$

where $y = {d}/{D}$ is the ratio of semi-major to semi-minor telescope dimensions. The SNR equation in terms of photon counts is defined as:

$$SNR = \frac{C_p}{\sqrt{C_p + 2C_b}}, \qquad (13)$$

where C_p is the counts from the planet and C_b is the counts from the noise background. The factor of 2 in the denominator arises from the dither maneuver and the differencing of two images used to eliminate speckle. The noise counts in Brown (2005) were converted to fluxes using equation (12) in order to later solve for integration time. There are noise contributions (components of C_b) from zodiacal light flux (both earth and exo-zodi), background speckle flux, dark counts and read noise. The read noise contribution is a constant, independent of integration time.

The flux over the bandpass for the planet is defined as:

$$F_p = F_0\left[10^{-\frac{V_{mag} + \Delta Mag}{2.5}}\right]T_{tot}\Delta\lambda \qquad (14)$$

where $F_0 = 9500$ photons cm^{-2} nm^{-1} sec^{-1} corresponds to the V-band specific flux for a zero magnitude star, V_{mag} is the visual magnitude of the observed star and ΔMag is the sensitivity limit.

The theoretical peak of the point spread function associated with a stellar observation is given by:

$$I_{PSF} = \frac{1}{y}\pi\frac{\left(D\cdot 10^9\right)^2}{4\lambda^2}, \qquad (15)$$

and the solid angle of a detector pixel (in steradians) is:

$$\Omega = y\left(\frac{\lambda}{2D\cdot 10^9}\right)^2. \qquad (16)$$

The flux for the associated background starlight speckles is therefore given by:

$$F_{bs} = F_0\left[10^{\frac{-V_{mag}}{2.5}}\right]\varsigma I_{PSF}n_x\Omega T_{tot}\Delta\lambda, \qquad (17)$$

where n_x represents noise pixels term associated with sharpness and ς is the uniform contrast level, which is the ratio of suppressed starlight to unsuppressed starlight (see Table 1 for values). The noise contribution from zodiacal light is given by:

$$F_{bz} = F_0 \left[10^{\frac{-M_{zodi}}{2.5}} \right] (1 + 2z) n_x \frac{\Omega}{4.848 \cdot 10^{-6}} T_{tot} \Delta\lambda \,. \qquad (18)$$

In the Brown model, z is the brightness of the exo-zodiacal light. The exo-zodiacal dust is assumed to be uniform in density and brightness. It is also assumed that an observation looks through the exo-zodi twice, so a factor of two is added to the Brown formulation. The flux contribution due to dark noise is given by:

$$F_{bd} = \frac{\xi n_x}{A} \qquad (19)$$

where ξ is the dark count rate. The contribution from read noise is given by:

$$C_{br} = 2R^2 n_x \,, \qquad (20)$$

where R is the read noise, which is independent of integration time. All of the terms except C_{br} are associated with integration time and may be converted into fluxes. Thus, the SNR equation becomes:

$$SNR = \frac{F_p A \tau}{\sqrt{F_p A \tau + 2(F_{bs} A \tau + F_{bz} A \tau + F_{bd} \tau + C_{br})}} \qquad (21)$$

Solving for integration time, τ, yields:

$$\tau = \max \left(\frac{-\alpha_2 + \sqrt{\alpha_2^2 - 4\alpha_1 \alpha_3}}{2\alpha_1}, \frac{-\alpha_2 - \sqrt{\alpha_2^2 - 4\alpha_1 \alpha_3}}{2\alpha_1} \right) \qquad (22)$$

where:

$$\alpha_1 = F_p^2 A \qquad (23)$$

$$\alpha_2 = -SNR^2 \left(F_p A + 2 \left(F_{bs} A + F_{bz} A + F_{bd} \right) \right) \qquad (24)$$

$$\alpha_3 = SNR^2 C_{br} \,. \qquad (25)$$

This integration time formulation is for one exposure and one rotation. For multiple rotations and observations, τ is multiplicatively increased by the number of rolls, dithers and visits. Since the planet flux is dependent on Δmag (through F_p, eq. 14), integration time varies with Δmag as shown in Fig. 4.
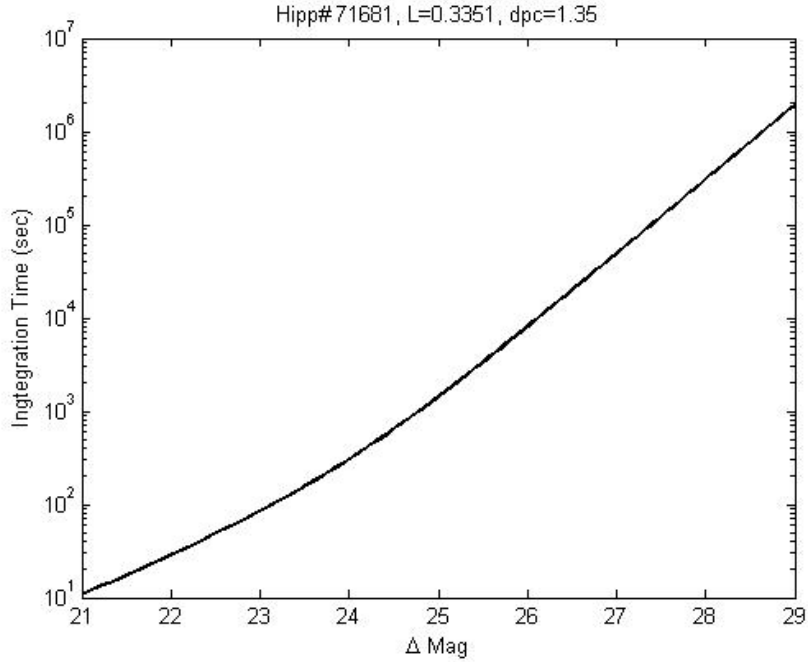
Fig. 4. Integration time curve. The curve has an approximately exponential rise increasing with Δmag.

4. OPTIMIZATION

The TPF-C visit program must be optimized in order to obtain the most benefit (largest total accumulated completeness) for the time spent observing. Without optimization, the visit strategy may be arranged based on the limiting requirements of the mission. This would imply observing all stars up to the Δmag sensitivity limit as shown by the red dots in Fig. 5. The stars may then be ranked by efficiency, where efficiency is defined as:

$$efficiency = \frac{Completeness}{\tau}. \tag{26}$$

The stars selected for the TPF-C program are those N with the highest efficiency that also fit within an integration time limit. The total integration time is given by:

$$\tau_m \leq \sum_{i=1}^{N} \tau_i \tag{27}$$

where τ_i is the time of observation for each star. We choose the mission time limit to be $\tau_m = 1$ year, as representative of integration time available during a three year mission. By varying the Δmag sensitivity (the height of the box in Fig. 2), curves for integration times vs. sensitivity are obtained for every candidate star (examples are depicted in Fig. 5). Completeness values at given integration times may be computed using the curves for completeness vs. Δmag (an example is shown Fig.3) and τ vs. Δmag (an example is shown in Fig. 4). A plot of completeness vs. τ is shown in Fig. 5 for two stars with different luminosities.
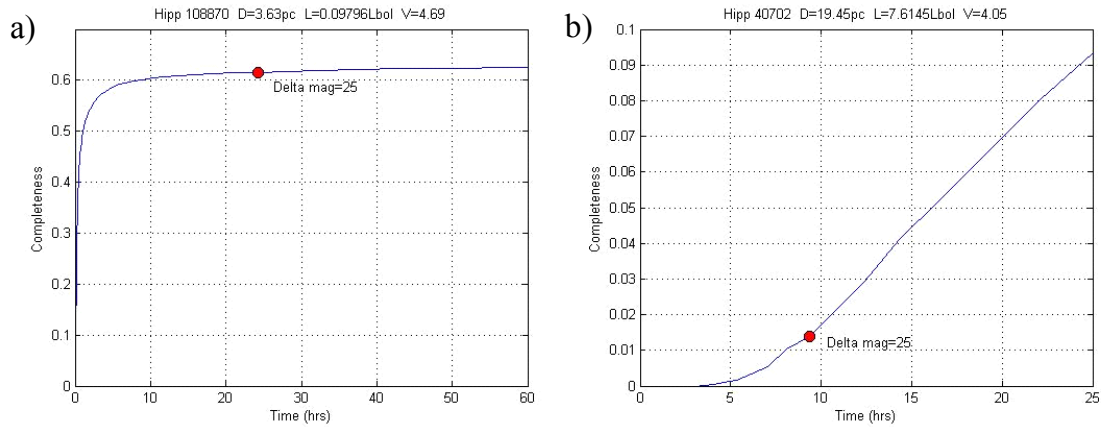
Fig. 5. Plots of completeness vs. integration time. a) Completeness curve for a lower luminosity star. b) Completeness curve for a high luminosity star. The red points indicate the point of limiting Δmag.

The completeness curves for lower luminosity stars, whose habispheres are generally poorly resolved due to their small physical size, begin to level off at longer integration times because the obscurational completeness limit is rapidly attained at small Δmag. As a result, little completeness gain is possible from observing to higher Δmag (see Fig. 6). The visit strategy may be optimized by moving the point of observation along the curve from right to left, cutting time off of the unproductive parts of the completeness curve (the right side).
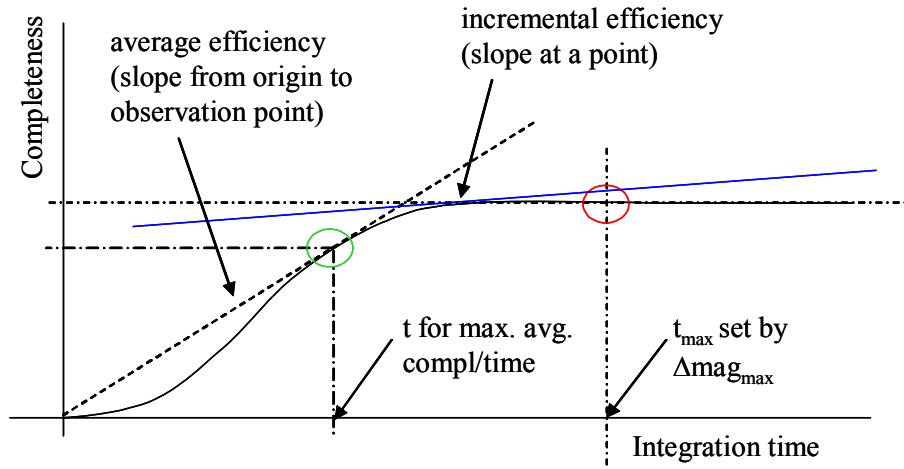

Fig. 6. Average completeness optimization diagram. The red circle indicates the point of observation for the limiting Δmag sensitivity case and the green circle indicates the point of observation for observing a star to its maximum average efficiency. The blue line is tangent to the slope of the curve, indicating the incremental efficiency at the point of tangency.

Vanderbei (2005) proposed one method of optimization in which each star is observed to the point of maximum average completeness per time (green circle in Fig 6). If all stars were identical, this would maximize overall efficiency. After observing to this point, the integration is then stopped for every star. Since all the stars in the optimization are not identical, the stars are sorted by best average efficiency. The list of stars whose cumulative integration time is less than τ_m is then selected for observation.

Another optimization method involves integrating until a fraction of completeness at limiting Δmag is achieved (depicted by the different color lines in Fig. 7). This fractional observation limit is iterated over a range of values from (50%, 90%) of the limiting Δmag. The integration is then stopped and the stars are sorted based on average efficiency with the new observation time. The candidate stars whose cumulative integration time is less than τ_m are then selected for observation.
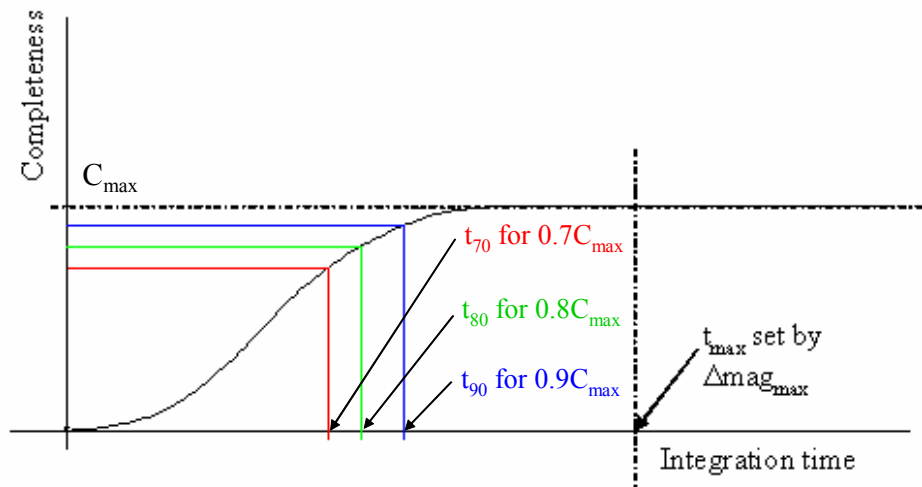

Fig. 7. Completeness cutoff optimization diagram. Integration is stopped when the curve reaches a fraction of the maximum completeness.

Both of the previous methods performed worse than the non-optimized case for limiting Δmag and therefore are not desirable techniques. However there are two methods which performed better than the limiting Δmag case. These are the auction and the efficiency threshold cutoff optimization methods.

4.1 Auction

Auction optimization was first presented by Brown (May, 2005). This method seeks to optimize the cumulative completeness by optimizing the time spent observing each star using the most productive portions of the completeness curve.

The first step in this optimization process is to obtain completeness curves for all candidate stars by observing up to the limiting Δmag (as shown by the red dot in Fig. 5). A star then "bids" its least efficient (last) hour of integration time. The hour of the lowest bidder (least efficient of the entire list) is then cut from the right side of the completeness curve (as depicted in Fig. 8a). This elimination, or auction, occurs over the whole star list, one star and hour at a time. A star is permitted to participate in the auction until it bids out all of its hours.
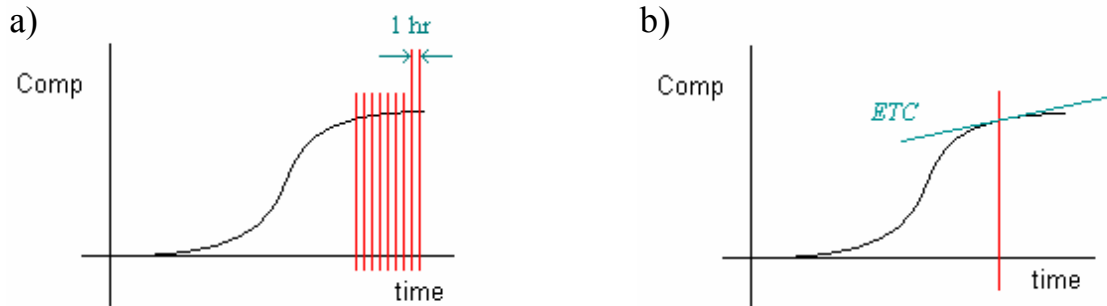

Fig. 8. Auction optimization vs. efficiency threshold cutoff (ETC) optimization for a given star a) Auction optimization cuts integration time hour by hour (an hour is cut for each of the red lines) based on the time which is least efficient. b) Efficiency threshold cutoff optimization eliminates the portion of the curve to the right of the red line, which is above an ETC.

In Fig. 8a, each of the red lines represents an auctioned cut of one hour of integration time. This auction eliminates integration time from stars until a time goal is met. Figure 9 shows a block diagram of the auction process.

Fig. 9. Auction diagram for single visit completeness.

The auction begins by setting an initial value for T_{cut}, the number of hours to be auctioned from the full list. Then the list of stars with corresponding completeness curves is read into the program. The integration time is reduced, one hour at a time, as shown in Fig. 8a, until a time goal (T_{cut}) is met. The stars are then sorted from highest to lowest efficiency and the set of stars, $A_N(T_{cut})$ satisfying equation (27) is kept. After iterating T_{cut} over a range from 0 (no hours cut) to T_{limit} (τ_m minus T_{cut}), the set A_N with highest total completeness is selected. In this way, the auction provides an optimization of single visit completeness over both average efficiency and auctioned time. This optimization method performs better than the non-optimized limiting Δmag case. Results are presented in sect. 5.

4.2 Efficiency Threshold Cutoff Optimization

An equivalent optimization technique method involves the use of an efficiency threshold cutoff (ETC). In this optimization method completeness curves are discretized into incremental efficiency steps (Brown's auction does not require this step). Each incremental efficiency step is defined as:

$$incremental\ efficiency = \frac{\Delta Completeness}{\Delta \tau}, \qquad (28)$$

where $\Delta \tau$ is given in hour increments and $\Delta Completeness$ is the completeness over a given hour of integration time. Incremental efficiency, therefore, defines the slope of the completeness curve for increments of $\Delta \tau$. In ETC optimization, integration times are reduced until the incremental efficiency is at or above the efficiency threshold cutoff. A diagram of this procedure is shown in Fig. 10.

Fig. 10. Efficiency threshold cutoff optimization diagram for single visit completeness.

The optimization process begins by setting a value for ETC instead of setting a value for T_{cut} as in the auction optimization. A list of stars and their corresponding completeness curves is then read into the program. All time that has an incremental efficiency below the ETC is cut from the right side of the completeness curves (as depicted in Fig 8b). The stars are then sorted by highest to lowest efficiency and the set of stars, $A_N(ETC)$ satisfying equation (27) is kept. After iterating ETC over a range from 0 (no hours cut) to ETC_{max} (the efficiency cutoff associated with cutting enough time to reach τ_m), the set A_N with highest total completeness is selected. Like the auction, this optimization combines the incremental and average efficiencies to obtain an optimized visit timing that is better than the non-optimized case.

Both auction and ETC optimizations produce equivalent results (see sect. 5) as both methods cut integration time based on incremental efficiency and then optimize over average efficiency. The efficiency threshold cutoff optimization, however, uses only one iteration, over ETC, instead of two iterations as in the auction case. It therefore runs faster, and thus was employed for future program completeness work.

5. RESULTS

The two different optimizations described in sections 4.1 and 4.2 give comparable results, which are shown in Table 2. There is a substantial benefit from increasing the sensitivity requirement from Δmag=25 to Δmag=26, as evident in Table 2.

	ETC		Auction	
ΔMag	# Stars	# Planets	#Stars	#Planets
25	138	32.60	135.21	32.59
25.5	125	38.29	122.77	38.32
26	115	41.10	113	40.96
27	114	42.16	106	41.04

Table 2. Comparison of results over a range of Δmag for the two different optimization methods.

In Table 2, #Stars is the number of targets observed in one year and #Planets is equivalent to the total accumulated completeness. The #Stars values for the auction were interpolated when the limit of one year of integration time fell between two stars. In order to directly compare to values produced by Brown, the values in Table 2 were computed with the throughput parameters given in Brown (2005). The case for the new throughput parameters, consistent with the current baseline optical prescription (Table 1), is shown in Fig. 11.
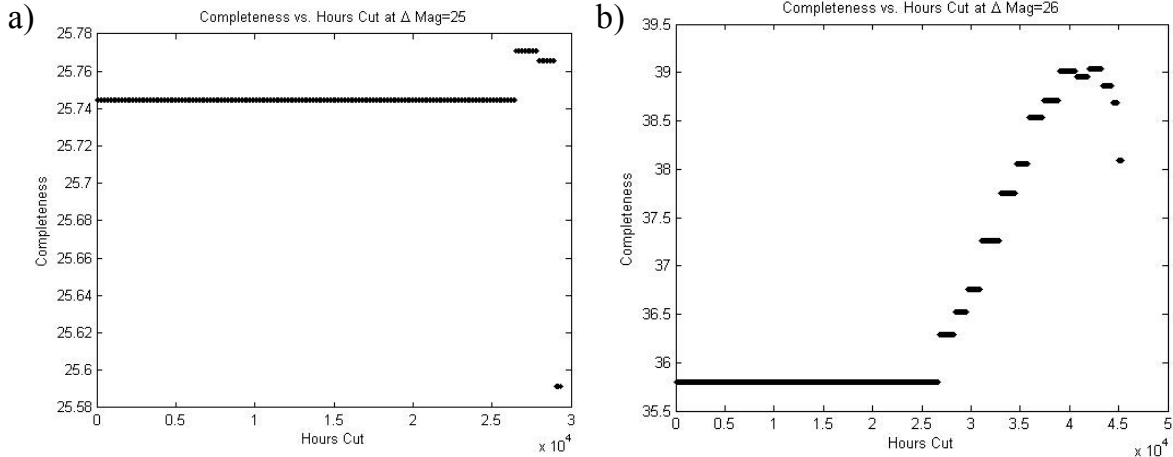
Fig. 11. Auction completeness optimization for different sensitivity limits. The long dark line indicates the completeness for the limiting Δmag case, where we employ the current baseline throughput parameters (Table 1).

In Fig. 11a and 11b, zero hours cut is equivalent to the Δmag limiting case where all stars are observed to the maximum Δmag (25 for 11a and 26 for 11b). Figure 11a shows that there is minimal gain from the non-optimized limiting case. However, Fig. 11b shows that for the Δmag = 26 case, there is a substantial increase in the completeness from both the baseline at Δmag = 26 (the dark line in Fig. 11b) and the maximum of the Δmag = 25 (the highest bar in Fig. 11a) case.

This simulation demonstrates that increasing the sensitivity requirements allows for more scientific gain (Fig. 11b shows approximately 50% more habitable zones searched than in Fig. 11a), while reducing the number of star searched (Table 2). However, since this optimization is based on a single visit, these results could change with the addition of multiple visits for a given star in a program completeness optimized program.

6. CONCLUSIONS

Completeness is a measure of how well the TPF-C mission meets its scientific requirement of planet detection. Completeness versus integration time curves are obtained for all possible candidate stars by relating completeness, instrument sensitivity (Δmag) and integration time. These curves are used to determine an optimized single visit strategy for TPF-C. The non-optimized case has all observations extending to the Δmag sensitivity limit. The visit strategy can be optimized by looking at how eliminating inefficient portions of the completeness curve for the visited.

We have explored several optimized strategies for maximizing completeness for the TPF-C mission and have demonstrated two different, but equivalent, optimization techniques that perform better than the non-optimized limiting Δmag case. The results from the auction and ETC optimization techniques indicate that increasing the sensitivity requirement allows for a large increase in the total accumulated completeness. Future work on completeness should take into account multiple visits to a star along with strategic and tactical factors which affect mission development and planning (Brown, July, 2005).

Acknowledgments

Special thanks to D. Palacios for editing assistance.

References:

Brown, R. A. "Buy-Back Auction optimization of TPF-C exposure times for first-visit completeness," (memo) May 23, 2005.

Brown, R. A. "Obscurational Completeness," ApJ **607**:1003-1013, 2004.

Brown, R. A. "Photometric and Obscurational Completeness," ApJ, 2005.

Brown, R.A. "Whole Mission Simulation – First Cut_2" (memo) July 9, 2005.

STDT. "Terrestrial Planet Finder Science Requirements," Version 2.3, September, 8 2005.

Vanderbei, R. "Maximizing Completeness in Observational Planning," (memo) 2005.

http://www.phy6.org/stargaze/Smotion.htm

http://www.frostydrew.org/observatory/courses/orbits/booklet.htm